

Synthesis and densification of W–30 wt%Cu composite powders using ammonium meta tungstate and copper nitrate as precursors

M. Ardestani*, H. Arabi, H.R. Rezaie, H. Razavizadeh

Department of Materials and Metallurgical Engineering, Iran University of Science and Technology, Narmak, Tehran 16846-13114, Iran

ARTICLE INFO

Article history:

Received 27 December 2008

Accepted 27 January 2009

Keywords:

W–Cu composites
Precipitation
Calcination
Sintering

ABSTRACT

W–30 wt%Cu composite powders were prepared by a novel precipitation process using ammonium meta tungstate and copper nitrate as precursors. The initial precipitates were obtained by adding aqueous ammonia to a mixture of ammonium meta tungstate and copper nitrate solutions and then heating the solution up to 95 °C. In order to synthesis W–Cu composite powders, the dried precipitates were calcined in air at 500 °C and then reduced by hydrogen. The calcination temperature was determined by thermogravimetry analysis. The powders were characterized by X-ray diffraction technique and scanning electron microscopy analysis. The effect of sintering temperature was investigated on densification of the synthesized powders. Relative density over 98% was achieved for the samples which were sintered at 1150 °C. Good electrical conductivity and relatively high hardness were achieved for the samples which sintered above melting point of copper.

© 2009 Elsevier Ltd. All rights reserved.

1. Introduction

W–Cu composites are widely used as arcing tips, resistance welding electrodes, electrode materials for electro discharge machining, heat sink materials for microelectronics packaging and materials in MHD (magnetohydrodynamics) power generation systems. These groups of composites combine the high hardness, hot strength and wear resistance of tungsten with the outstanding electrical and thermal conductivity of copper [1–3]. Generally, these composites are produced by copper infiltration of tungsten performs. However, this technique is not a net shape process and does not result to a homogeneous microstructure [4]. Moreover, it is known that W–Cu composites hardly reach full density without addition of a small amount of other elements such as Co and Ni as sintering aids. But these elements deteriorate electrical and thermal conductivity of W–Cu composites [5,6]. In recent years, synthesis of W–Cu composites has been investigated by sintering W–Cu composite powders. In these kinds of powders, without adding any additives nearly dense and homogenous composites could be fabricated due to fine dispersion of copper and tungsten. Several methods like mechanothermochemical [7] mechanical alloying [8] and mechanochemical [9] were used to synthesis W–Cu composite powders so far. However, the mentioned techniques, especially the last two ones include long time ball milling and the powders could be contaminated during the process. Contamination causes a decrease in conductivity after sintering the powder compacts [10,11].

In this study, in order to synthesis W–Cu composite powders, ammonium meta tungstate and copper nitrate were used as raw materials. The introduced synthesizing procedure does not include mechanical milling so the prepared powders would not be contaminated from the milling media. Also, the effect of sintering temperature on consolidation, electrical conductivity and hardness of the powders was investigated.

2. Experimental

White colored ammonium meta tungstate-AMT ($H_{26}N_6O_{40}W_{12}$ -aq, >99.0% purity, Fluka, Germany) and blue colored copper nitrate ($Cu(NO_3)_2 \cdot 3H_2O$, >99% purity, Merck, Germany) were used as raw materials. In order to synthesis W–30 wt%Cu composites, AMT and copper nitrate solutions were made separately in distilled water. Subsequently, the two solutions added to each other and heated at about 80 °C. Then for each 100 cm³ of the solution 3 cm³ aqueous ammonia were added to the solution. By heating the solution up to 95 °C, ammonia evaporated completely and green precipitates formed. Worth mentioning that after the first filtration of the solution, the above mentioned process (i.e. adding ammonia, heating and filtering the solution) should be repeated until the solution became completely colorless. In this condition, pH was in the range of 5–6. Then the obtained precipitates in each step, washed, dried and simple mixed.

In order to determine the appropriate calcination temperature, the dried precipitates were subjected to thermogravimetry analysis (TGA) (NETZSCH STA 409 PC/PG) up to 750 °C with a heating

* Corresponding author. Tel.: +98 22413892; fax: +98 2177240480.
E-mail address: mohammadard@yahoo.com (M. Ardestani).

rate of $10\text{ }^{\circ}\text{C min}^{-1}$ in air atmosphere. The precipitates calcined at $500\text{ }^{\circ}\text{C}$ for 2 h. The calcined precipitates reduced at $850\text{ }^{\circ}\text{C}$ for 3 h in hydrogen atmosphere (dew point $-76\text{ }^{\circ}\text{C}$) in a tube-type electrical furnace. The powders were characterized by X-ray diffraction (XRD) technique (XRD–Jeol8030–Cu $K\alpha$). The reduced powders were uni-axially compacted at a pressure of 200 MPa. The powder compacts sintered in a tube-type electrical furnace in hydrogen with a heating rate of $10\text{ }^{\circ}\text{C min}^{-1}$ to $1000\text{--}1150\text{ }^{\circ}\text{C}$ for 1.5 h. The densities of the sintered samples were determined by Archimedes method. The electrical conductivity of the sintered powders was evaluated by four probe DC method. Also, the hardness of the sintered specimens measured by a Vickers hardness tester. The morphologies of the powders and the microstructure of the sintered samples were observed by scanning electron microscopy (SEM, Cambridge S360).

3. Results and discussion

3.1. Synthesis of W–Cu composite powders

Fig. 1 shows the SEM micrograph of the initial dried precipitates. This figure shows the precipitates have near spherical shapes and have been partially agglomerated.

The thermogravimetry of the initial precipitates up to $750\text{ }^{\circ}\text{C}$ in air atmosphere is shown in Fig. 2. According to this figure, the weight loss of the precipitates occurs up to $500\text{ }^{\circ}\text{C}$ and above this temperature no changes is detectable in TG curve. This result shows that the volatile constituents such as water and ammonia evaporated completely after heating at $500\text{ }^{\circ}\text{C}$.

The XRD pattern of the calcined precipitates at $500\text{ }^{\circ}\text{C}$ is shown in Fig. 3. According to this pattern, the calcined precipitates consisted of CuWO_{4-x} phase. Therefore, one can conclude that the appropriate temperature for calcination of the initial precipitates is $500\text{ }^{\circ}\text{C}$. SEM micrograph of the calcined powders is shown in Fig. 4. This figure shows that due to evaporation of the volatile compounds, the calcined powders have a different morphology compared to initial precipitates. Also, according to this figure, the calcined powder has been agglomerated. Calcination at higher temperatures may result to further agglomeration of the particles.

The XRD pattern of the reduced powders is shown in Fig. 5. This pattern shows the reduced powders consisted of W and Cu phases. SEM micrograph of these powders is presented in Fig. 6. This figure shows that the particles are approximately worm shape and have submicron size.

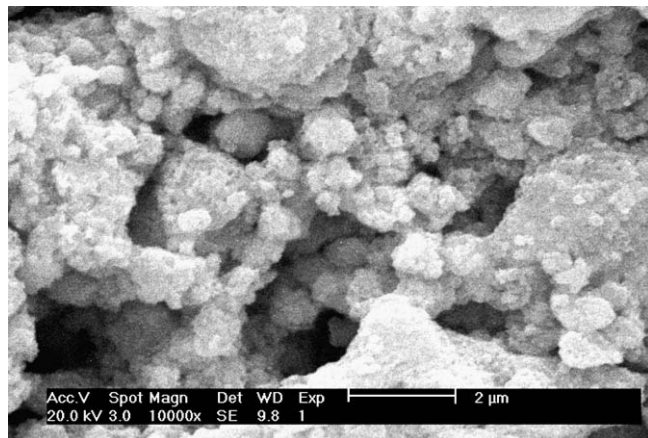


Fig. 1. SEM micrograph of the initial dried precipitates.

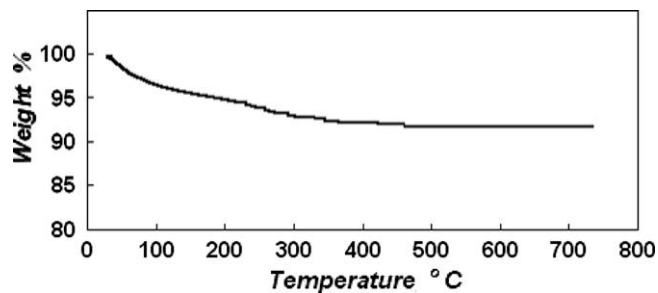


Fig. 2. TG curve of the initial precipitates up to $750\text{ }^{\circ}\text{C}$ in air.

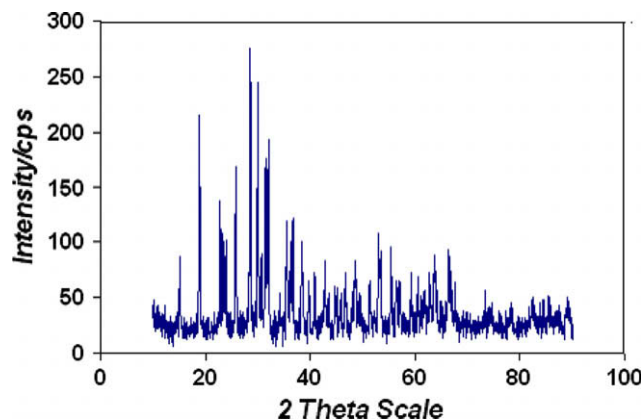


Fig. 3. XRD pattern of the calcined powders at $500\text{ }^{\circ}\text{C}$. The pattern shows only CuWO_{4-x} peaks.

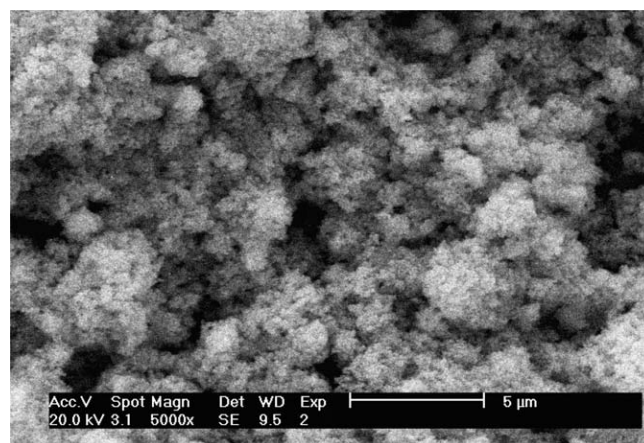


Fig. 4. SEM micrograph of the calcined powders at $500\text{ }^{\circ}\text{C}$.

3.2. Densification of the reduced powders

The effect of sintering temperature on the relative density and diametral shrinkage of the samples is shown in Fig. 7. The measured relative densities of the sintered specimens at 1000 , 1100 and $1150\text{ }^{\circ}\text{C}$ are 72.12, 96.7 and 98.08%, respectively. Also, diametral shrinkages of the samples at these temperatures are 6, 15.5 and 17.5%, respectively. Therefore one may conclude that melting of copper has significant influence on consolidation of the sintered samples $T_{m\text{Cu}} = 1083\text{ }^{\circ}\text{C}$. However, according to the results, increasing of sintering temperature at about $1100\text{ }^{\circ}\text{C}$ has not a considerable effect on the increase of relative density of the compacts, but with increasing the temperature the density is improved.

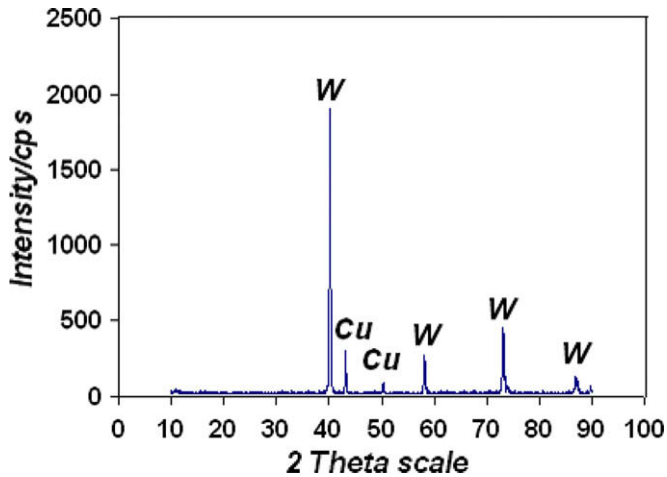


Fig. 5. XRD pattern of the reduced powders.

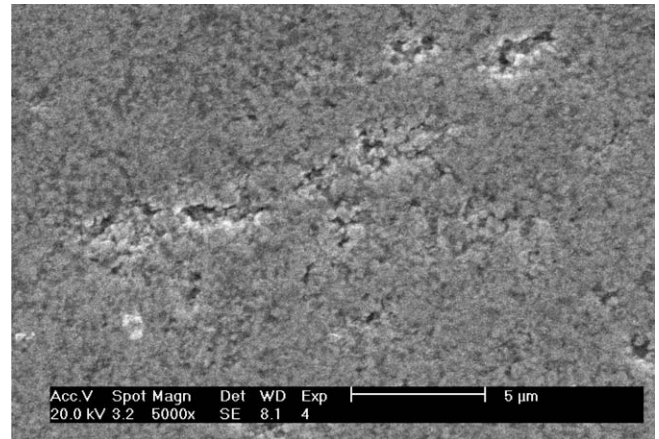


Fig. 8. SEM micrograph of the samples sintered at 1000 °C for 1.5 h.

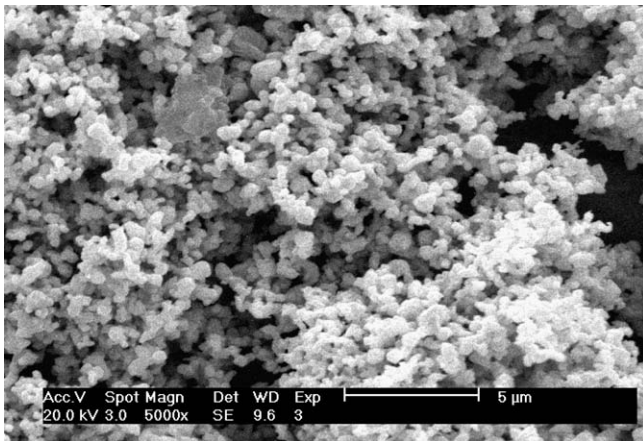


Fig. 6. SEM micrograph of the reduced powders.

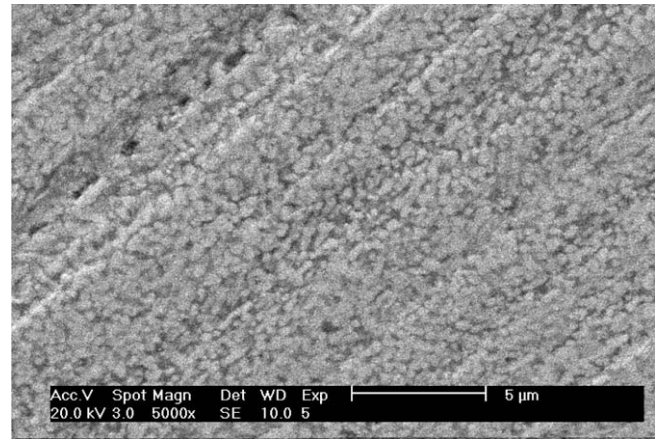


Fig. 9a. SEM image of the sintered samples at 1100 °C.

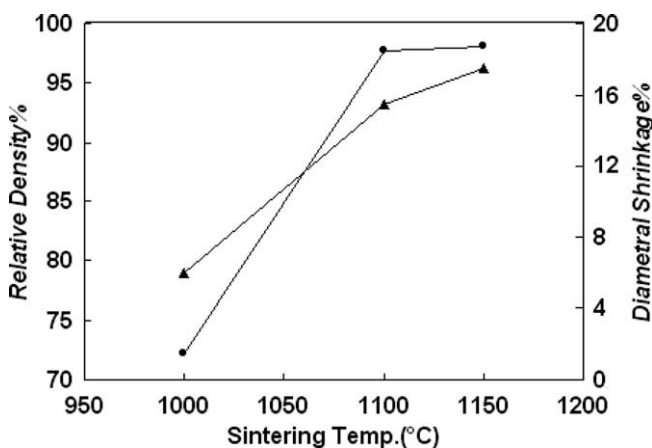


Fig. 7. Relative densities and diametral shrinkages of the samples versus sintering temperature. The theoretical density is 14.33 g cm^{-3} .

Below melting point of copper, solid state sintering is the main mechanism for densification of W–Cu compacts. During solid state sintering, diffusion of copper from the bulk of the composite particles resulted to formation of Cu necks between the composite particles. This phenomenon favors densification in solid state sintering according to Refs. [12,13]. The SEM micrograph of the sintered

samples at 1000 °C is shown in Fig. 8. This figure shows partially sintered microstructure of W–Cu composite.

Above 1083 °C, liquid phase sintering was responsible for densification of the compacted powders. In general, densification during liquid phase sintering occurs through a combination of particle rearrangement due to capillary forces, grain shape accommodation by solution re-precipitation and sintering of tungsten by solid state diffusion [14]. In the case of W–Cu composites, the low solubility of tungsten and copper makes the contribution of solution re-precipitation negligible, so the dominant mechanism for densification seems to be the rearrangement of W particles. Similar observation has been reported by other researchers [14,15]. The main restriction for rearrangement is the bonds between tungsten particles which form during heating and sintering the compacts. The rearrangement of W particles occurs when the W skeleton network is weaker than the capillary forces according to Johnson et al. [14]. In the case of synthesized powders, although fine particles contributes to stronger W–W bonds, but the fine distribution of Cu and W phases increase the capillary forces which helps rearrangement of W phases during liquid phase sintering. Figs. 9a and 9b show the SEM images of the sintered specimens at 1100 and 1150 °C.

3.3. Electrical conductivity and hardness of the sintered samples

Fig. 10 shows the effect of sintering temperatures on electrical conductivity (in the term of percentage of International Annealed

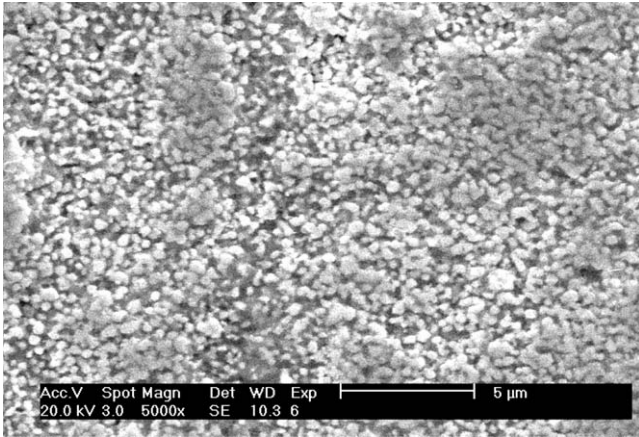


Fig. 9b. SEM image of the sintered samples at 1150 °C.

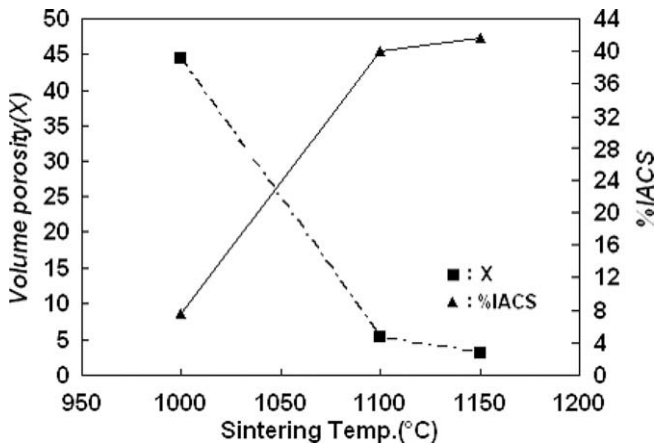


Fig. 10. The effect of sintering temperature on conductivity (reported as percentage of International Annealed Copper Standard) and volume porosity of the sintered samples.

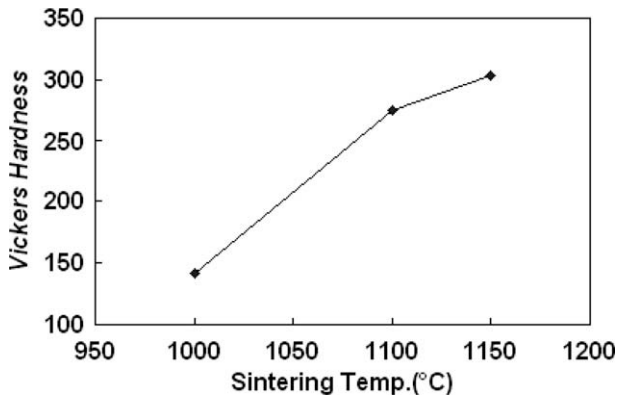


Fig. 11. Vickers hardness versus sintering temperature for the samples sintered at different temperatures.

Copper Standard – % IACS) and volume fraction porosity (X) of the sintered samples. The volume fraction porosity of the samples can be calculated as below [16]

$$X = \frac{d_{th} - d_c}{d_{Cu}} \quad (1)$$

where d_{th} , d_c and d_{Cu} are the theoretical composite density (14.33 g cm^{-3}), measured composite density and pure copper density (8.96 g cm^{-3}), respectively. As it shown in this figure, by increasing the sintering temperature the electrical conductivity of the samples enhanced to 41.7% IACS due to decrease in the volume fraction of porosities. The theoretical electrical conductivity of this composite is about 45% IACS [17].

The effect of sintering temperature on hardness of the sintered specimens is shown in Fig. 11. The hardness of the sintered samples at 1000, 1100 and 1150 °C is 142, 275 and 303 Vickers, respectively. This should be related to higher relative density of the samples which have been sintered at elevated temperatures. It is worthy to note that the hardness of the composites which were produced by conventional methods is 150 HB [1] which is approximately half of the hardness of the synthesized composite.

4. Conclusion

W–30 wt%Cu composite powders synthesized via precipitation method using ammonium meta tungstate and copper nitrate as raw materials. The process includes precipitation of W–Cu compounds, calcination of the initial precipitates in air, and reduction of the calcined powders in hydrogen atmosphere. Due to fine distribution of tungsten and copper phases, the synthesized powders showed good sinter ability and high relative density especially after sintering above melting point of copper. Over 300 Vickers hardness and 41.7% IACS electrical conductivity obtained for the sintered samples at 1150 °C.

Acknowledgement

The authors would like to appreciate from Materials and Energy Research Centre (MERC) for their financial support.

References

- [1] Lassner E, Schubert W. Tungsten. New York: Kluwer Academic Publishers; 1999.
- [2] Davis JR. Copper and copper alloys (ASM Specialty Handbook): ASM International; 2001.
- [3] Zhao N, Li J, Yang X. Influence of the P/M process on the microstructure and properties of WC reinforced copper matrix composite. *J Mater Sci* 2004;39:4829–34.
- [4] Li Y, Qu X, Zheng Z, Lei C, Zou Z, Yu S. Properties of W–Cu composite powder produced by a thermo-mechanical method. *Int J Refract Met Hard Mater* 2003;21:259–64.
- [5] Kim DG, Kim GS, Oh ST, Kim YD. The initial stage of sintering for W–Cu nanocomposite powder prepared from W–CuO mixture. *Mater Lett* 2004;58:578–81.
- [6] Moon IH, Kim EP, Petzow G. Full densification of loosely packed W–Cu composite powders. *Powder Metall* 1998;41:51–7.
- [7] Hong SH, Kim BK. Fabrication of W–20wt%Cu composite nanopowder and sintered alloy with high thermal conductivity. *Mater Lett* 2003;57:2761–7.
- [8] Kim JC, Moon IH. Sintering of nanostructured W–Cu alloys prepared by mechanical alloying. *Nanostruct Mater* 1998;10:283–90.
- [9] Kim DG, Lee BK, Oh ST, Young DK, Kang SG. Mechanochemical process for W–15wtCu nanocomposite powders with WO_3 –CuO powder mixture and its sintering characteristics. *Mater Sci Eng* 2005;395A:333–7.
- [10] Cheng J, Song P, Gong Y, Cai Y, Xia Y. Fabrication and characterization of W–15Cu composite powders by a novel mechano-chemical process. *Mater Sci Eng* 2008;488A:453–7.
- [11] Yoon ES, Lee JS, Oh ST, Kim BK. Microstructure and sintering behavior of W–Cu nanocomposite powder produced by thermo-chemical process. *Int J Refract Met Hard Mater* 2002;20:201–6.
- [12] da Costa FA, da Silva AGP, Gomes UU. The influence of the dispersion technique on the characteristics of the W–Cu powders and on the sintering behavior. *Powder Technol* 2003;134:123–32.
- [13] Ryu SS, Kim YD, Moon IH. Dilatometric analysis on the sintering behavior of nanocrystalline W–Cu prepared by mechanical alloying. *J Alloys Compd* 2002;335:233–40.

- [14] Johnson JL, Berzovsky JJ, German RM. Effects of tungsten particle size and copper content on densification of liquid-phase-sintered W–Cu. *Metall Mater Trans* 2005;36A:2807–14.
- [15] Kim JC, Ryu SS, Kim YD, Moon IH. Densification behavior of mechanically alloyed W–Cu composite powders by the double rearrangement process. *Scripta Mater* 1998;39:669–76.
- [16] Deshpande PK, Li JH, Lin RY. Infrared processed Cu composites reinforced with WC particles. *Mater Sci Eng* 2006;429A:58–65.
- [17] Honga SH, Kima BK, Munir ZA. Synthesis and consolidation of nanostructured W-10-40wt%Cu powders. *Mater Sci Eng* 2005;405 A:325–32.